03-002

MODELLING OF A HEAT EXCHANGER FOR A SPOUTED BED BASED PILOT PLANT

Sukunza Pérez, Xabier; Aguado Zarraga, Roberto

UPV/EHU

Although the spouted bed technology was first developed for drying of granulate solids, it has been used for thermal processes such as pyrolysis, gasification, combustion and drying of suspensions. The temperature and air flow rates of these processes vary in a wide range. Thus, the present work aims designing and modelling a versatile heat exchanger for the implementation of a gas burner into a multi-purpose spouted bed technology based pilot plant.

Design procedure begins with the estimation of the temperature of the combustion gases in the burner, which has been validated by means of literature references. This value is used together with maximum pressure for material selection and design parameters. Considering the operation conditions for all the applications, the exchange area for heat transfer has been established for maximum energy requirement, 800 Nm3/h and 450 ºC, which gives the dimensions of the heat exchanger.

The dynamic model involves the estimation of the overall heat transfer coefficient and pressure drop. Thus, the model has been used for simulating different fuels, air flow rates and heat exchange areas in order to assess that any application considered can be carried out in the pilot plant.

Keywords: *design; modelling; heat exchanger; conical spouted bed*

MODELADO DE UN INTERCAMBIADOR DE CALOR PARA PLANTA PILOTO DE LECHO EN SURTIDOR

Aunque la tecnología de lecho en surtidor fue inicialmente desarrollada para el secado de materiales granulares, ha sido utilizada para procesos térmicos como la pirólisis, combustión, gasificación y secado de suspensiones. Las temperaturas y caudales utilizados en estos procesos varían en un amplio rango, por tanto este trabajo tiene como objetivo diseñar y modelar un intercambiador de calor para la adaptación de un quemador de gas en una planta piloto spouted bed.

El diseño comienza con la estimación de la temperatura de los gases de combustión en el quemador, la cual ha sido validada. Este valor ha sido utilizado junto con la presión máxima para la elección del material y parámetros de diseño. Considerando las condiciones de operación de todas las aplicaciones se ha estimado el área máximo de intercambio para el máximo requerimiento energético, 800 Nm3/h y 450 ºC, logrando así las dimensiones del intercambiador.

El modelo dinámico implica el cálculo del coeficiente global de transferencia de calor y la pérdida de carga. Así, el modelo ha sido utilizado para la simulación de diferentes combustibles, caudales de aire y áreas de intercambio para garantizar que cualquier aplicación puede llevarse a cabo en la planta piloto.

Palabras clave: *diseño; modelado; intercambiador de calor; lecho en surtidor cónico*

Correspondencia: Xabier Sukunza x.sukunza.perez@gmail.com

Acknowledgements/Agradecimientos: I would like express my very great appreciation to Professor Roberto Aguado, my research supervisor, for his patient guidance and constructive criticism in the present work. I would also like to thank Dr. Aitor Pablos and Aitor Kortina for their willingne

1. Introduction

The Catalytic Processes and Waste Valorisation Research group (University of the Basque Country, UPV/EHU) aims the study and development of waste valorisation processes such as pyrolysis, gasification and combustion of synthetic and natural polymers and drying of granulate solids and suspensions. To this end, the research group suggests the spouted bed due to its advantages over other thermal treatment technologies.

The spouted bed was first developed by Mathur & Gishler (1954) for drying of granulate solids as an alternative to fluidised beds due to high energetic efficiency under certain conditions. However, conventional spouted bed (a cylinder with a conical base) presents several restrictions involving its scaling up: adhesive solids tend to form agglomerations due to small particle movement and inlet diameter should be no more than 60 times the particle size in order to assure bed stability (Olazar et al. 1993).

Thus, Olazar et al. (1992) developed the conical spouted bed in order to overcome those challenges. However, in both conventional and conical spouted beds, increasing bed height turns into high bed heterogeneity and instability, hindering spouted bed operability. The use of internal devices, such us draft-tubes, overcomes these geometrical limitations and allows handling Geldart B type particles (Geldart 1973), increasing spouted bed versatility (Altzibar et al. 2008; Altzibar et al. 2013; Altzibar et al. 2013).

Since draft-tube partially supports bed weight and reduces bed pressure drop, particle velocity increases at the fountain, which leads into higher fine particle entrainment probability. Fountain confinement internal device was proposed by the Research group, which is located on the surface of the bed and forces the particles to return to bed annulus, considerably reducing particle entrainment. Air trajectory is also modified, since it goes up until it reaches upper zone of the fountain confiner and descends through the wall, creating a counter current flow between particle and air, thus mass and energy transfer are improved (Pablos et al. 2018).

This configuration, conical spouted bed with fountain confinement device and draft-tube, has been proven to be very effective for solid thermal treatment such us combustion (San José, Alvarez & López 2018), gasification (Lopez et al. 2017; Cortazar et al. 2018), pyrolysis (Artetxe et al. 2010; She & Dong 2015), torrefaction (Wang et al. 2017), polymerisation (Olazar et al. 1994) and drying (Altzibar et al. 2007; Altzibar et al. 2008; Pablos 2017), due to multiple advantages, including high turbulence, high solid recirculation, high mass and energy transfer and high homogenisation bed properties (Pallai, Szentmarjay & Mujumdar 2014).

2. Objectives

The present work is framed in the joint project of Catalytic Process & Waste Valorisation Research group, (University of the Basque Country, UPV/EHU) and Novattia Desarrollos Ltd., technology Development Company, with the objective of commercialising spouted bed based pilot plants, processes and equipment.

Presently, the consortium owns a spouted bed based pilot plant for drying of fine and ultrafine sands. Therefore, due to all the promising results of the Research group, the aim of the consortium is to adapt the actual pilot plant for pyrolysis, combustion, torrefaction and drying of suspensions. Temperature and air flow rates of these processes vary in a wide range. Therefore, the present work aims designing and modelling a versatile heat exchanger for the implementation of a gas burner into a multi-purpose spouted bed pilot plant. For that, the following milestones have been proposed:

- Estimation and validation of combustion gases temperature in the burner
- Material selection and shell, tubes, flanges and insulation thickness estimation
- Prediction of operation conditions of the processes considered in the present work
- Estimation of the maximum heat exchange surface area for the highest energy requirement
- Modelling for the simulation of the proposed processes in order to validate the designed heat exchanger

3. Methodology

3.1. Preliminary calculations

Gas burner implementation involves designing a heat exchanger that supplies gas flow rates at the required temperature. Since in the processes proposed combustion gases from the burner cannot directly be fed into the chamber, the present work suggests designing a counter current shell-tube heat exchanger. In order to avoid manufacturing and experiments expenses, a mathematical model is developed in order to carry out some simulations that will validate the designed heat exchanger, Figure 1.

Figure 1. Algorithm flow diagram for modelling and simulation of the burner and the exchanger

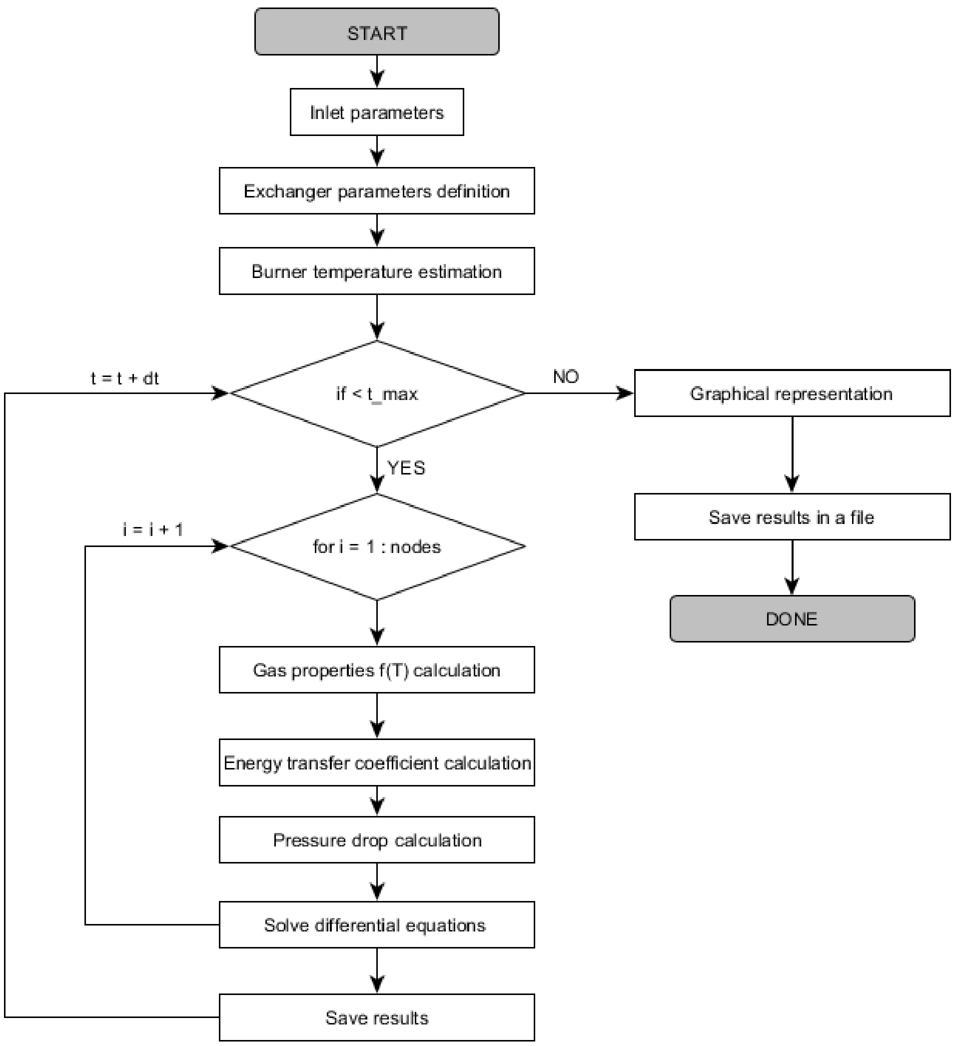

Firstly, the algorithm estimates the composition and temperature of the combustion gases in the gas burner, which allows natural gas and LPG as fuels. For that, fuel flow rate is previously calculated by eq. (1), and considering that manufacturing company establishes stoichiometric coefficient at 1.15, air flow rate may be estimated.

$$Q_g = \frac{P}{\eta_{burn} f LHV} \tag{1}$$

Where Q_g is the fuel volumetric flow rate, P is the power of the burner, η_{burn} is the efficiency of the burner (75%), f is the correction factor, which is given by manufacturing company, and LHV is the Low Heating Value of the fuel.

In order to simplify simulation iteration time, total combustion of fuel is contemplated, thus composition of combustion gases is given by the following reactions:

$$CH_4 + 2O_2 \rightarrow CO_2 + 2H_2O \tag{2}$$

$$C_2H_6 + \frac{7}{2}O_2 \rightarrow 2CO_2 + 3H_2O \tag{3}$$

$$C_3H_8 + 5O_2 \rightarrow 3CO_2 + 4H_2O \tag{4}$$

$$C_4H_{10} + \frac{13}{2}O_2 \rightarrow 4CO_2 + 5H_2O \tag{5}$$

Estimation of combustion gases temperature considers gas burner efficiency, eq (6), defined as the amount of chemical energy used to heat the combustion gases to the outlet temperature. Maximum efficiency (100%) is obtained when combustion gases reach flame adiabatic temperature, that is, chemical energy of reactants will not been wasted.

$$\eta_{burn} = \frac{H_{prod} - H_{react}}{HHV} \tag{6}$$

3.2. Differential equations

In the heat exchanger hot gas (service) flows through the shell, while cold gas (process) flows through the internal tubes. In order to maximise heat transfer coefficient, service gases flow perpendicularly to the internal tubes, thus internal baffles are designed to modify trajectory of service gas. The algorithm defines a node as the space between baffles, in which gas properties do not change. In addition, in order to simplify calculation time, chemical reactions and temperature of combustion gases are considered constant over time. Therefore, mass and energy balances are neglected in the burner. However, although in the heat exchanger mass balances are negligible, the model does consider energy balances in each node. The node is divided in three regions: 1) internal tubes, 2) space between tubes and shell wall and 3) shell wall and insulation.

As the flow rate of the gas process is equally distributed to each tube, enthalpy balance is defined in a single tube, which contemplates inlet and outlet process gas convective enthalpies and heat transfer to the shell region, eq (7). Enthalpy balance in the space between shell wall and tubes considers inlet and outlet service gas convective enthalpies, heat transfer from the gas to the tubes and heat loss to insulation, eq (8). Finally, eq (9) contemplates enthalpy balance at the shell, that is, heat transfer from service gas to insulation and natural convection loss to the ambience.

$$\frac{dT_{tub}^{(n)}}{dt} = Q_{tub}^{(n+1)} C_{p,tub}^{(n+1)} \rho_{tub}^{(n+1)} T_{tub}^{(n+1)} - Q_{tub}^{(n)} C_{p,tub}^{(n)} \rho_{tub}^{(n)} T_{tub}^{(n)} + UA_{tub}\left(T_{shell}^{(n)} - T_{tub}^{(n)}\right) \tag{7}$$

$$\frac{dT_{shell}^{(n)}}{dt} = Q_{shel}^{(n-1)} C_{p,shell}^{(n-1)} \rho_{shell}^{(n-1)} T_{shel}^{(n-1)} - Q_{shell}^{(n)} C_{p,shell}^{(n)} \rho_{shell}^{(n)} T_{shell}^{(n)} - UA_{tub}\left(T_{shell}^{(n)} - T_{tub}^{(n)}\right) - UA_{ins} n_t \left(T_{shell}^{(n)} - T_{ins}^{(n)}\right) \quad (8)$$

$$\frac{dT_{ins}^{(n)}}{dt} = UA_{ins}\left(T_{shell}^{(n)} - T_{ins}^{(n)}\right) - h_{amb}\left(T_{ins}^{(n)} - T_{amb}\right) \quad (9)$$

Enthalpy of the first node in the shell region depends on enthalpy supply of the burner, and enthalpy of the last node in the tube region depends on enthalpy supply of the blower. Moreover, gas properties, heat transfer coefficients and pressure drop are estimated in each node in order to solve the equations.

Viscosity, specific heat coefficient and thermal conductivity coefficients have been calculated by means of NIST chemical database for every compound.

Global heat transfer coefficients have been calculated for heat transfer between shell and tube regions, and shell and insulation regions. The first coefficient considers forced convection from service gas to the wall of internal tubes, heat conduction through wall of the tubes and forced convection from the tube to process gas, eq (10).

$$UA_{tub} = \frac{1}{h_{tub,int} a_{tub} + \frac{\ln(D_{tub}/d_{tub})}{2\pi k_{tub} \Delta L} + h_{tub,ext} A_{tub}} \quad (10)$$

Eq (11) gives global heat transfer coefficient between shell and insulation regime, in which three heat transfer types are differentiated: forced convection in the shell, conduction through the shell wall and conduction through the insulation wall.

$$UA_{ins} = \frac{1}{h_{shell} A_{shell} + \frac{\ln(D_{shell}/d_{shell})}{2\pi k_{shell} \Delta L} + \frac{\ln(D_{ins}/d_{ins})}{2\pi k_{ins} \Delta L}} \quad (11)$$

Convection and conduction coefficients, together with natural convection from the insulation surface to the ambience, have been calculated using Nusselt number based correlations (Çengel 2007).

The algorithm also estimates service and process gas pressure drop through the heat exchanger, since pressure determines gas density and volumetric flow rate in each node. Pressure drop in the internal tubes is neglected since the heat exchanger has been designed with straight tubes. However, due to the installation of baffles, service gas will modify its trajectory, and therefore, pressure drop must be taken into account. Gaddis & Gnielinski (1997) proposed specific equations have been used in the present work in order to estimate pressure drop in baffle type heat exchangers.

4. Results

4.1. Temperature of combustion gases in the burner

Some simulations have been carried out for different burner powers and fuels, Figure 2. Combustion of natural gas reaches temperatures up to 1340 ºC, while combustion of LPG reaches 1385 ºC due to differences in LHV. These values remain constant over burner power, since fuel quantity and supplied air balance up.

4.2. Material selection

Selected material for manufacturing the heat exchanger must bear operation conditions, that is, high temperature resistance and contrasts at the beginning of the experiment, high pressures, and reactive atmosphere. Therefore, the following properties must be considered:

- Physical: high thermal conductivity and low thermal expansion coefficient
- Mechanical: good deformation, failure, fatigue and hardness properties
- Corrosion: High corrosion resistance
- Manufacturing: Easiness for shaping and welding
- Economical: Minimum cost

Ordinary and refractory steels and nickel-chrome alloys have been dismissed due to high temperatures values. TZM (molybdenum, titanium, zirconium and carbon alloy) has been selected for shell, baffles, tubes and flanges due to high conduction and low expansion coefficients and low costs over other materials, including iron-chrome (KANTHAL) and molybdenum-hafnium (MHC) alloys.

4.3. Estimation of heat exchange area

Table 1 shows operation conditions of the processes considered in the future pilot plant. Theoretical power (P_{theo}) to heat the process gas up to the required temperature at the outlet of the exchanger has been estimated for all the processes.

Table 1. Operation conditions of the considered processes

Keyword	Q (Nm3/h)	T (ºC)	P_{theo} (kW)
Catalytic pyrolysis	50	600	11.62
Thermal pyrolysis	80	600	18.60
Torrefaction	100	300	10.90
Sand drying	100	450	19.14
Paste like drying	290	300	31.63
Rice shell combustion	300	400	45.07
Olive waste combustion	300	500	57.42
Low temperature suspensions drying	430	300	46.60
High temperature suspensions drying	430	500	82.30
Low temperature industrial sand drying	800	300	87.26
High temperature industrial sand drying	800	450	136.66

Heat exchanger sizing involves the estimation of the heat exchange surface area at the most adverse condition: high temperature industrial sand drying (800 Nm^3/h and 450 ºC), eq (12).

$$A_{tub}^{tot} = \frac{q_{exch}}{U_{exc}\ \Delta T_{LM}} \tag{12}$$

where U_{exch} is the global heat transfer coefficient, estimated in 10 $Wm^{-2}K^{-1}$ (Çengel 2007) and q_{exch} is the exchange energy rate, which gives service gas outlet temperature, 522 ºC, by eq. (13), yielding 78.95 m^2 of exchange area. Natural gas has been used for calculations, since lower temperature is reached in heat exchanger inlet.

$$q_{exch} = Q_{shell}\rho_{shell}C_{p,shell}\Delta T_{shell} = Q_{tub}\rho_{tub}C_{p,tub}\Delta T_{tub} \tag{13}$$

4.4. Heat exchanger design

Since the exchanger must fit in the space in the pilot plant, 4 m length and 1 m diameter have been established as maximum dimensions for the exchange area. DN50 type tubes (Ø60.3 mm) have been selected as internal tubes, since these kind of tubes are commonly used in metal manufacturing, which will reduce manufacturing costs. In addition, triangular pattern is used for location of internal tubes, giving a more robust heat exchanger and hence, the heat exchanger sizing is optimised. As a result, 103 internal tubes have been estimated for the construction of the heat exchanger.

In order to assure tube holding and to modify service gas trajectory through the exchanger, 9 baffles have been designed, giving 10 nodes of simulation, whose dimensions are shown in Figure 2. Service gas inlet and outlet are situated at the top of the exchanger, which facilitates the exhaust to the chimney. Process gas inlet has been designed according to the blower connection pipe dimensions. In addition, it has been located at the bottom of the exchanger connected to a previous tank in order to assure homogeneous distribution of the gas before entering to the tubes. Process gas leaves the tubes in another tank, which acts as gas collector. This tank has an outlet connection in order to connect the heat exchanger to the pilot plant.

Figure 2. Internal baffles dimensions in mm

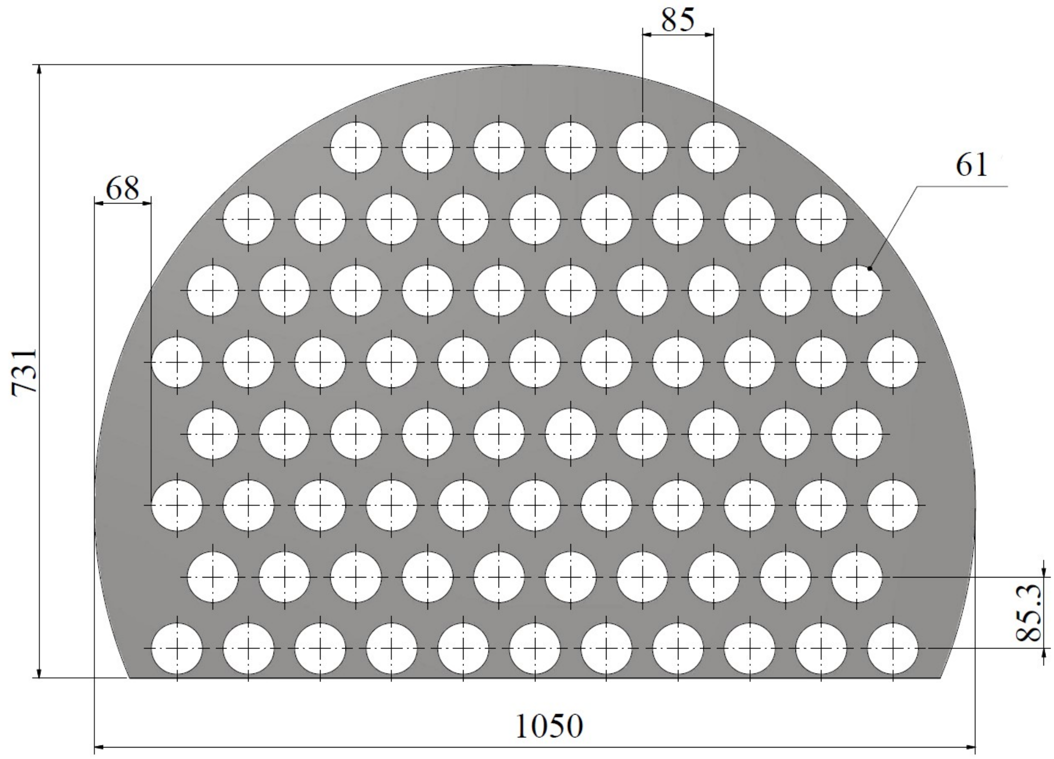

Figure 3. Horizontal and vertical views of the heat exchanger. Dimensions in mm

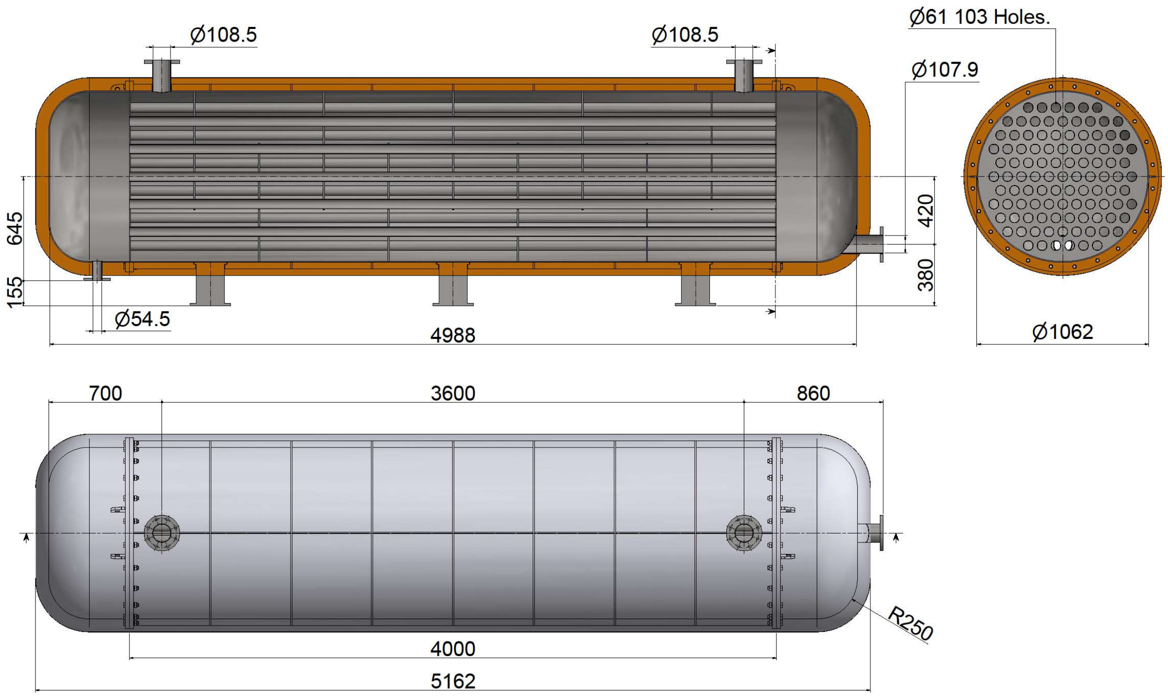

4.5. Simulation results

As a dynamic model has been developed, process gas temperature evolution over time will be shown for different temperature levels, as well as some steady state parameters, including burner power, P_{burn}, number of tubes, n_t, chimney temperature, T_{chim} and heat exchanger efficiency, η_{exch}. The latter is defined as enthalpy gain of the process gas over the inlet enthalpy of service gas.

The aim of the simulations is to optimise the number of tubes in order to reduce energy waste. Firstly, the use of all the tubes is simulated and, in case energy requirement is lower than the minimum burner power, 35 kW, the number of tubes are reduced. Moreover, in some cases tube-power combinations do not converge during algorithm simulation, hence both parameters may be changed until reaching a convergent solution.

Since the conclusions drawn from all the simulations are similar, the most relevant results will be shown in this work in order to understand heat exchanger's behaviour. Table 2 shows steady state results for process gas outlet temperature of 300 ºC using gas natural as fuel. Figure 4 shows dynamic results for these conditions. Higher burner power is needed for higher energy requirements. As minimum burner power is 35 kW, at lower demanding conditions the burner has proven to be oversized, giving high chimney temperatures. At higher energy requirements and, although minimum burner power is used, the number of internal tubes increases, giving lower chimney temperature and thus higher exchanger efficiencies.

Table 2. Results for process gas outlet temperature of 300 ºC using natural gas as fuel

Q (Nm^3/h)	P_{theo} (kW)	P_{burn} (kW)	n_t	T_{chim} (ºC)	η_{exch} (%)
100	10.9	35	7	921	24.9
290	31.6	35	67	288	70.9
430	46.9	50	103	253	74.1
800	87.3	100	87	348	68.9

Dynamic results show that at higher process gas volumetric flow rate, time needed by the system to reach steady state is reduced, since 1) more fuel is required, thus higher inlet enthalpy is introduced to the exchanger and 2) increasing gas velocities Reynolds and therefore Nusselt number values increase.

Table 3 shows steady state results when LPG is used as fuel for same process gas outlet temperature. In most cases, burner power required is lower due to higher LHV over natural gas, although at 800 Nm^3/h the results differ at same operation conditions. As explained before, when gas natural is used as fuel, a convergent result could not be achieved with lower burner power and maximum tubes required, while the algorithm does reach a convergent solution with LPG.

Table 3. Results for process gas outlet temperature of 300 ºC using LPG as fuel

Q (Nm^3/h)	P_{theo} (kW)	P_{burn} (kW)	n_t	T_{chim} (ºC)	η_{exch} (%)
100	10.9	39	11	974	22.5
290	31.6	35	66	281	69.9
430	46.9	48	103	230	73.9
800	87.3	86	103	193	77.0

Process gas temperature evolution over time reveals that slightly more time is required by the system in order to reach steady state, since at lower burner power service gas residence time in the exchanger is larger, reducing heat transfer.

Figure 4. Process gas outlet temperature evolution over time for different volumetric flow rates. Process temperature: 300 ºC for a) natural gas and b) LPG

a)

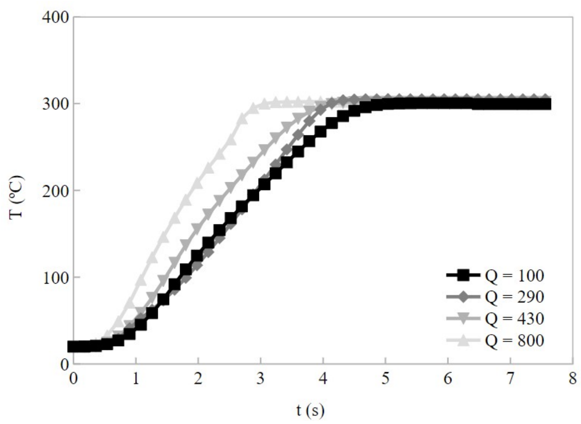

b)

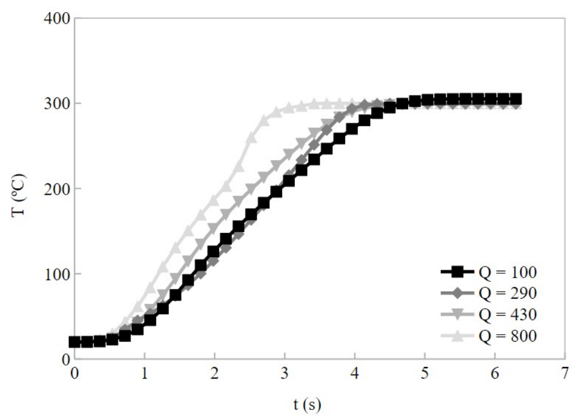

Table 4 shows steady state results for process gas outlet temperature of 450 ºC using natural gas as fuel. Maximum energy requirement is shown in this result, 800 Nm^3/h and 450 ºC, which has been used for heat exchanger sizing. Both burner power (190 kW) and chimney temperature (559 ºC) are similar to design values (200 kW and 522 ºC).

Table 4. Results for process gas outlet temperature of 450 ºC using natural gas as fuel

Q (Nm^3/h)	P_{theo} (kW)	P_{burn} (kW)	n_t	T_{chim} (ºC)	η_{exch} (%)
100	17.1	40	22	833	37.5
800	136.7	190	103	559	55.5

Although heat exchanger design has been validated for every operation condition, exchange efficiency is not high enough in order to commercialise the proposed heat exchanger. However, as said before, the main objective was to design a versatile and flexible heat exchanger that could be able to supply the required gas volumetric flow rate and temperature to the spouted bed contactor.

5. Conclusions

A heat exchanger has been designed, modelled and simulated for the adaptation of a gas burner to a multi-purpose spouted bed technology based pilot plant. From the simulations the next conclusions have been drawn:

- The outlet temperature of the combustion gases at the outlet of the burner is large when LPG is utilised as fuel, due to its high heating value. It can also be concluded that with both natural gas and LPG, the temperature does not significantly change even for different values of power of the burner. In addition, the validation of the outlet temperature of the combustion gases has been carried out by means of references from the literature.
- The usage of a special metallic alloys for shell, tubes and flanges of the exchanger is recommended in this work, since the maximum operation temperature is up to 1385 ºC. Several alloys have been compared and TZM alloy has been selected due to its good mechanical, physical and manufacture properties and low cost.
- The validation of the designed model has been accomplished, since it reaches the proposed steady state temperature of the process fluid in all cases considered in between 4 and 7 s. Therefore, the response of the designed system is faster than the response of custom electrical heaters and thus, the operations costs are reduced.
- The present work does not consider the optimisation of the exhaust chimney temperature of the service fluid, which, in many cases, gives low efficiency values. In order to increase the efficiency of the system the integration of the gas burner and heat exchanger in the pilot plant for other processes, such as heating the inert up in endothermic pyrolysis reactions, could be done.

6. References

Altzibar, H., Lopez, G., Alvarez, S., San Jose, M.J., Barona, A. & Olazar, M., 2008, 'A draft-tube conical spouted bed for drying fine particles', *Drying Technology*, 26(3), 308–314.

Altzibar, Haritz, Lopez, G., Bilbao, J. & Olazar, M., 2013, 'Effect of draft tube geometry on pressure drop in draft tube conical spouted beds', *The Canadian Journal of Chemical Engineering*, 91(11), 1865–1870.

Altzibar, H., Lopez, G., Estiati, I., Bilbao, J. & Olazar, M., 2013, 'Particle Cycle Times and Solid Circulation Rates in Conical Spouted Beds with Draft Tubes of Different Configuration', *Industrial & Engineering Chemistry Research*, 52(45), 15959–15967.

Altzibar, H., Lopez, G., San Jose, M.J., Alvarez, S. & Olazar, M., 2007, 'Drying of Fine Sand in a Pilot Plant Unit Provided with a Draft-Tube Conical Spouted Bed', *Chemical Engineering Transactions*, 11, 725–730.

Artetxe, M., Lopez, G., Amutio, M., Elordi, G., Olazar, M. & Bilbao, J., 2010, 'Operating conditions for the pyrolysis of poly-(ethylene terephthalate) in a conical spouted-bed reactor', *Ind. Eng. Chem. Res.*, 49(5), 2064–2069.

Çengel, Y., 2007, *Heat and mass transfer. A practical approach*, 2nd edn., McGraw-Hill, New York.

Cortazar, M., Alvarez, J., Lopez, G., Amutio, M., Santamaria, L., Bilbao, J. & Olazar, M., 2018, 'Role of temperature on gasification performance and tar composition in a fountain enhanced conical spouted bed reactor', *Energy Conversion and Management*, 171, 1589–1597.

Gaddis, E.S. & Gnielinski, V., 1997, 'Pressure drop on the shell side of shell-nad-tube heat exchangers with segmental baffles', *Chemical Engineering and Processing*, 36, 149–159.

Geldart, D., 1973, 'Types of gas fluidization', *Powder Technology*, 7(5), 285–292.

Lopez, G., Cortazar, M., Alvarez, J., Amutio, M., Bilbao, J. & Olazar, M., 2017, 'Assessment of a conical spouted with an enhanced fountain bed for biomass gasification', *Fuel*, 203, 825–831.

Mathur, K.B. & Gishler, P.E., 1954, *A technique of contacting gases with coarse solid particles. Preprint of a paper to be presented at a Meeting of the American Institute of Chemical Engineers at Glenwood Springs, Colorado, Sept. 13, 1954*, Ottawa, Ont.

Olazar, M., San, J., Aguayo, A.T., Arandes, J.M. & Bilbao, J., 1992, 'Stable operation conditions for gas-solid contact regimes in conical spouted beds', *Industrial and Engineering Chemistry Research*, 31(7), 1784–1792.

Olazar, M., San, J., Penas, F.J., Aguayo, A.T. & Bilbao, J., 1993, 'Stability and hydrodynamics of conical spouted beds with binary mixtures', *Industrial and Engineering Chemistry Research*, 32(11), 2826–2834.

Olazar, M., San, J., Zabala, G. & Bilbao, J., 1994, 'New reactor in jet spouted bed regime for catalytic polymerizations', *Chemical Engineering Science*, 49(24 PART A), 4579–4588.

Pablos, A., 2017, *Diseño de un contactor spouted bed para el secado de arenas finas y ultrafinas. Thesis for the University of the Basque Country.* – PhD thesis, Leioa .

Pablos, A., Aguado, R., Tellabide, M., Altzibar, H., Freire, F.B., Bilbao, J. & Olazar, M., 2018, 'A new fountain confinement device for fluidizing fine and ultrafine sands in conical spouted beds', *Powder Technology*, 328, 38–46.

Pallai, E., Szentmarjay, T. & Mujumdar, A., 2014, 'Spouted Bed Drying', in A.S. Mujumdar (ed.), *Handbook of Industrial Drying, Fourth Edition*, pp. 351–370, CRC Press.

San José, M.J., Alvarez, S. & López, R., 2018, 'Catalytic combustion of vineyard pruning waste in a conical spouted bed combustor', *Catalysis Today*, 305, 13–18.

She, Y. & Dong, F., 2015, *Spouted fluidized bed powdered coal pyrolysis device and method. Patente: CN105062529 (A)*, (CN20151569605 20150909).

Wang, Z., Lim, C.J., Grace, J.R., Li, H. & Parise, M.R., 2017, 'Effects of temperature and particle size on biomass torrefaction in a slot-rectangular spouted bed reactor', *Bioresource Technology*, 244, 281–288.